Clinical Cancer Research

Updated version	Access the most recent version of this article at: http://clincancerres.aacrjournals.org/content/16/24/6071
Supplementary Material	Access the most recent supplemental material at: http://clincancerres.aacrjournals.org/content/suppl/2011/01/02/16.24.6071.DC1.html

Cited Articles	This article cites by 40 articles, 10 of which you can access for free at: http://clincancerres.aacrjournals.org/content/16/24/6071.full.html#ref-list-1

E-mail alerts	Sign up to receive free email-alerts related to this article or journal.
Reprints and Subscriptions	To order reprints of this article or to subscribe to the journal, contact the AACR Publications Department at pubs@aacr.org.
Permissions	To request permission to re-use all or part of this article, contact the AACR Publications Department at permissions@aacr.org.

A Hypoxia- and α-Fetoprotein–Dependent Oncolytic Adenovirus Exhibits Specific Killing of Hepatocellular Carcinomas

Oh-Joon Kwon[1], Pyung-Hwan Kim[1], Steven Huyn[2], Lily Wu[2], Minjung Kim[1], and Chae-Ok Yun[1]

Abstract

Purpose: Oncolytic adenoviruses (Ad) constitute a new promising modality of cancer gene therapy that displays improved efficacy over nonreplicating Ads. We have previously shown that an E1B 19-kDa-deleted oncolytic Ad exhibits a strong cell-killing effect but lacks tumor selectivity. To achieve hepatoma-restricted cytotoxicity and enhance replication of Ad within the context of tumor microenvironment, we used a modified human α-fetoprotein (hAFP) promoter to control the replication of Ad with a hypoxia response element (HRE).

Experimental Design: We constructed Ad-HRE$_6$/hAFPΔ19 and Ad-HRE$_{12}$/hAFPΔ19 that incorporated either 6 or 12 copies of HRE upstream of promoter. The promoter activity and specificity to hepatoma were examined by luciferase assay and fluorescence-activated cell sorting analysis. In addition, the AFP expression- and hypoxia-dependent *in vitro* cytotoxicity of Ad-HRE$_6$/hAFPΔ19 and Ad-HRE$_{12}$/hAFPΔ19 was determined by 3-(4,5-dimethylthiazol-2-yl)-2,5-diphenyltetrazolium bromide assay and cytopathic effect assay. *In vivo* tumoricidal activity on subcutaneous and liver orthotopic model was monitored by noninvasive molecular imaging.

Results: Ad-HRE$_{12}$/hAFPΔ19 exhibited enhanced tumor selectivity and cell-killing activity when compared with Ad-hAFPΔ19. The tumoricidal activity of Ad-HRE$_{12}$/hAFPΔ19 resulted in significant inhibition of tumor growth in both subcutaneous and orthotopic models. Histologic examination of the primary tumor after treatment confirmed accumulation of viral particles near hypoxic areas. Furthermore, Ad-HRE$_{12}$/hAFPΔ19 did not cause severe inflammatory immune response and toxicity after systemic injection.

Conclusions: The results presented here show the advantages of incorporating HREs into a hAFP promoter–driven oncolytic virus. This system is unique in that it acts in both a tissue-specific and tumor environment–selective manner. The greatly enhanced selectivity and tumoricidal activity of Ad-HRE$_{12}$/hAFPΔ19 make it a promising therapeutic agent in the treatment of liver cancers. *Clin Cancer Res; 16(24); 6071–82. ©2010 AACR.*

Liver cancer is one of the most common types of malignant tumors worldwide. Unfortunately, the poor prognosis associated with this disease escalates it to third on the list of the most common causes of death from cancer (1), and hepatocellular carcinoma (HCC) is the most prevalent form of liver cancer. Importantly, HCC is known to be resistant to both chemotherapy and radiotherapy. There-

fore, alternative therapeutic strategies for treatment are needed (2, 3). Gene therapy has emerged as a treatment option for cancer in the last 15 years (4, 5). To date, adenoviral vectors account for the most common type of viral vector used both in cancer gene therapy and in gene therapy clinical trials (6). Many characteristics have contributed to the favorable status of adenoviruses (Ad) in their application toward cancer gene therapy (7–9). However, the preferential trafficking of Ad vectors to the liver has been postulated as a drawback in achieving efficient gene delivery *in vivo*. In previous studies, following systemic administration of the Ad in preclinical models, more than 95% of injected vectors were sequestered in the liver (10, 11). In this study, we explored the possibility of utilizing the dominant liver trafficking ability of Ad vectors to target cancer cells in the liver.

Oncolytic Ads represent a relatively novel cancer therapeutic agent. The ability to control viral replication and subsequent cancer cell lysis in a tumor-selective manner makes oncolytic therapy particularly attractive. Furthermore, the replication process enables progeny virion to achieve secondary infection, thereby expanding the therapeutic

Authors' Affiliations: [1]Brain Korea 21 Project for Medical Sciences, Institute for Cancer Research, Yonsei Cancer Center, Severance Biomedical Science Institute, Yonsei University College of Medicine, Seoul, Korea; and [2]Department of Molecular & Medical Pharmacology, School of Medicine, University of California, Los Angeles, California

Corresponding Authors: Chae-Ok Yun, Institute for Cancer Research, Severance Biomedical Science Institute, Yonsei University College of Medicine, 134 Shinchon-Dong, Seodaemun-Gu, Seoul, Korea. Phone: 82-2-2228-8040; Fax: 82-2-2227-7751; E-mail chaeok@yuhs.ac; or Lily Wu, School of Medicine, University of California, Los Angeles, CA 90095-1735. Phone: 310-794-4390; E-mail: lwu@mednet.ucla.edu

efficacy of the oncolytic virus. The result is a more effective therapeutic agent than the conventionally used replication-deficient Ad (12, 13). Our group has recently developed an oncolytic Ad devoid of the E1B 19-kDa protein (Ad-ΔE1B19) that exhibits effective cytolytic activity (14). However, one drawback to the use of Ad-ΔE1B19 is that it exhibits relatively weak tumor selectivity. Hence, a strategy to improve its therapeutic activity is to introduce stringent tumor-specific transcriptional regulatory elements to direct the viral replication, namely, the expression of E1A proteins (15).

Human α-fetoprotein (hAFP) is an important biomarker for HCC. It is a developmentally regulated gene whose activity decreases after birth and becomes undetectable in normal adult tissues. Interestingly, the *AFP* gene is reactivated to high levels in HCC. Elevated serum levels of AFP have been observed in more than 70% of HCC patients, making AFP a useful diagnostic and prognostic marker of HCC (16–18). Recently, Nakabayashi and colleagues developed a shortened form of the hAFP regulatory region [from −5.1 to −2.9 kb and the proximal minimal promoter (169 bp)] that exhibited strong transcriptional activity even in low AFP-expressing HCCs (19). On the basis of its cell-selective activity, we decided to use the modified hAFP promoter to regulate replication of our oncolytic Ads to target AFP-expressing HCCs. A potential drawback to the use of tissue-selective promoters, to direct *E1A* gene expression, is that it displays relatively weaker transcriptional activity than the strong constitutive promoter such as CMV (cytomegalovirus) and SV40 (Simian virus 40). To circumvent this obstacle, we incorporated tumor-selective control elements to augment viral replication. Although mammalian tissues exist at 2% to 9% oxygen (O_2) conditions, tumor environment is known to be hypoxic, exhibiting a median O_2 level of 1.3% (20, 21).

Hence, we integrated hypoxia response elements (HRE; ref. 22) into our oncolytic Ads in conjunction with the modified hAFP promoter in order to achieve more robust and selective cytotoxicity against HCCs.

In this report, we investigated the possibility of exploiting the dominant liver trafficking ability of Ad vectors as a treatment of HCCs. We constructed Ad-HRE$_6$/hAFPΔ19 and Ad-HRE$_{12}$/hAFPΔ19 oncolytic Ads that incorporated either 6 or 12 copies of HRE enhancers upstream of the hAFP promoter. We showed that the transcriptional strength and selectivity of the oncolytic virus were enhanced to achieve HCC-specific and tumor microenvironment–selective viral replication and tumor killing in cell culture experiments, as well as in preclinical liver tumor models. On the basis of this report, we foresee that the novel oncolytic Ad Ad-HRE$_{12}$/hAFPΔ19 can be a promising therapy for aggressive HCCs.

Materials and Methods

Cell lines and cell culture

The cell lines were purchased from American Type Culture Collection and were cultured in Dulbecco's modified Eagle's medium (Gibco BRL) or modified Eagle's medium (Gibco BRL) supplemented with 10% of fetal bovine serum (Gibco BRL), penicillin (100 IU/mL), and streptomycin (50 μg/ml). All cell lines were maintained at 37°C in a humidified incubator at 5% CO_2. Hypoxia was achieved using prewarmed aluminum hypoxic chambers evacuated through the use of 94% N_2/5% CO_2. Oxygen concentration was controlled to the desired levels of 1%.

Construction of replication-incompetent and -competent Ads

To construct the modified hAFP promoter, we obtained the pAF5.1[Δ2.7]-CAT plasmid from Dr. Tamaoki's group (University of Calgary, Alberta, Canada). The HRE fragment was obtained from the 5′-flanking region of the *VEGF* gene by PCR using primers 5′-TCGAGCCACAG-TGCATACGTGGGCTCCAACAGGTCCTCTTG-3′ and 3′-CGGTGTCACGTATGCACCCGAGGTTGTCCAGGAGAAC-AGCT-5′. The repeat of HRE was generated by the concatemerization of the PCR product. HREs were inserted upstream of the modified hAFP promoter to generate shuttle vectors for both replication-incompetent and -competent Ads. The shuttle vectors and p*vmdl*324*BstBI* were linearized with *Xmn*I and *Bst*BI and transformed into BJ5183 bacteria for homologous recombination to generate Ad plasmid vectors. All Ad plasmids were digested with *Pac*I and transfected and propagated in 293A cells. Virus was then purified using CsCl gradient. Ads were titered in 293A cells by using the TCID$_{50}$ method.

Fluorescence-activated cell-sorting analysis

To assess both the specificity and transcriptional activity of modified AFP promoters, fluorescence-activated cell sorting (FACS) analysis was carried out. Cells were infected with Ad-expressing green fluorescent protein (GFP) under

the control of modified AFP promoters at the indicated viral particles (VP) per cell (2,000 VPs/cell for Huh-7, Hep3B, and A549; 5,000 VPs/cell for Hep1 and CBHEL; 10,000 VPs/cell for BJ). At 48 hours postinfection, cells were harvested with dissociation solution (Sigma) and washed with PBS 3 times. GFP expression levels from each group were analyzed by FACScan (Beckton-Dickinson). Data were collected from 10,000 cells and analyzed with the CellQuest software (BD Biosciences Immunocytometry Systems).

Replication-incompetent Ads in human liver cancer

To establish Hep3B or Hep1 tumors, 1×10^7 cells of Hep3B or 5×10^6 cells of Hep1 were injected subcutaneously in the abdomen of 7-week-old male athymic nu/nu mice (Chungang Animal). When tumor volume reached about 200 mm^3, each animal received intratumoral injections of the vectors (5×10^9 VPs) for 3 consecutive days. At 4 days after last administration, tumors were collected, fixed in 10% formalin, and embedded in paraffin (Wax-it). Tumor sections were stained with anti-GFP monoclonal antibody (MAB3580; Chemicon).

Cytopathic effect assay

To evaluate the cytopathic effect (CPE) by oncolytic Ad infection, cells were plated onto 24-well plates, grown until approximately 40% to 80% confluent, and infected with Ad-ΔE1B19, Ad-hAFPΔ19, Ad-HRE$_6$/hAFPΔ19, or Ad-HRE$_{12}$/hAFPΔ19 at 20 to 10,000 VPs/cell. At 3 to 16 days postinfection, plates were gently washed with PBS and stained with 0.5% crystal violet in 50% methanol for 1 hour. Cells were then washed with water and dried.

MTT assay

To assess the cytotoxic effect of the virus, cells were seeded onto 24-well plates at 2×10^4 to 1×10^5 cells per well and infected with oncolytic Ads. Cells were incubated in hypoxia or normoxia. At the indicated times postinfection, 250 μL of MTT [3-(4,5-dimethylthiazolyl-2-yl)-2,5-diphenyltetrazolium bromide; Sigma] in PBS (2 mg/mL) was added to each well following media removal. Cells were then incubated for 4 hours at 37°C. The formed precipitates were then dissolved in 1 mL of dimethylsulfoxide. Cell viability was determined by measuring absorbance at 540 nm, using a microplate reader. Nontreated groups at each day were set as 100% viability.

Replication-competent Ads in human liver cancer

The Hep3B tumor was established as described previously. When tumor volumes reached 150 to 200 mm^3, each oncolytic Ad (5×10^9 VPs) was intratumorally administrated on days 0, 2, and 4. Tumor growth was assessed by caliper measurements, and the volume was calculated (Volume = $0.523 \times$ length $\times$ width^2). At 7 days post–final injection, tumors were collected. Sections were stained with anti-Ad polyclonal antibody (AB1056; Chemicon) and antipimonidazole monoclonal antibody (HP1-100; Chemicon).

Orthotopic model of human liver cancer

Hep3B cells (1×10^6), which stably express firefly luciferase, mixed with growth factor–containing Matrigel (BD Bioscience) were injected into the left liver lobe of athymic nude mice (Charles River). At 15 days postimplantation, blood was harvested by retro-orbital bleeding, and AFP level was analyzed by ELISA (R&D Systems). When the level of AFP expression reached approximately 300 ng/mL, mice were divided into 3 separate groups in order to receive systemic treatment of PBS, 1×10^{10} VPs of Ad-hAFPΔ19 or Ad-HRE$_{12}$/hAFPΔ19 ($n = 7$, each group). Blood was collected at days 0 and 32. Optical imaging was carried out on days 0, 11, 18, 25, and 32 with IVIS SPECTRUM (Xenogen). Imaged signals were quantitatively analyzed with IGOR-PRO Living Image software (Xenogen). At 32 days after first treatment, tumors were collected, imaged, weighed, and finally sectioned. The E1A, hexon, and pimonidazole were detected from sections and then processed for fluorescent staining by Alexa fluor 568 goat anti-rabbit IgG (Invitrogen), Alexa fluor 488 goat anti-mouse IgG (Invitrogen), or Alexa fluor 568 rabbit anti-goat IgG (Invitrogen), respectively.

The measurement of inflammatory cytokine and toxicity studies

The inflammatory immune response and toxicity were examined after systemic injection of PBS ($n = 7$), 2×10^{10} VPs of Ad-ΔE1B19 ($n = 7$), or Ad-HRE$_{12}$/hAFPΔ19 ($n = 7$). At 6 hours postinjection, serum was harvested by retro-orbital bleeding and analyzed to detect interleukin 6 (IL-6) level (DY406; R&D System). At 3 days posttreatment, mice were sacrificed and blood and organs (liver, spleen, kidney, stomach, muscle, heart, and lung) were obtained. From serum, the aspartate aminotransferase (AST) and alanine aminotransferase (ALT) levels were determined. Examination for toxicity was carried out by BIOTOXTECH Corporation. The harvested organs were sectioned, and representative sections were stained by hematoxylin and eosin (H&E).

Statistical analysis

The data are shown as mean $\pm$ SE. Statistical comparison was made using Stat View software (Abacus Concepts) and the Mann–Whitney test (nonparametric rank-sum test). The criterion for statistical significance was taken as $P < 0.05$.

Results

Selective and increased GFP expression by HREs

To confirm the selectivity of the hAFP promoter and assess the impact of incorporating HREs, we assayed the reporter activities of HREs/hAFP combination in plasmids (Supplementary Fig. 1A) and replication-incompetent Ads (Fig. 1A). The hAFP promoter was active only in AFP-positive HCCs (Huh-7 and Hep3B). Moreover, the combined use of HREs with the hAFP promoter resulted in increased expression in hypoxia (Supplementary Fig. S1B). Figure 1B shows the transcriptional activity of hAFP- or
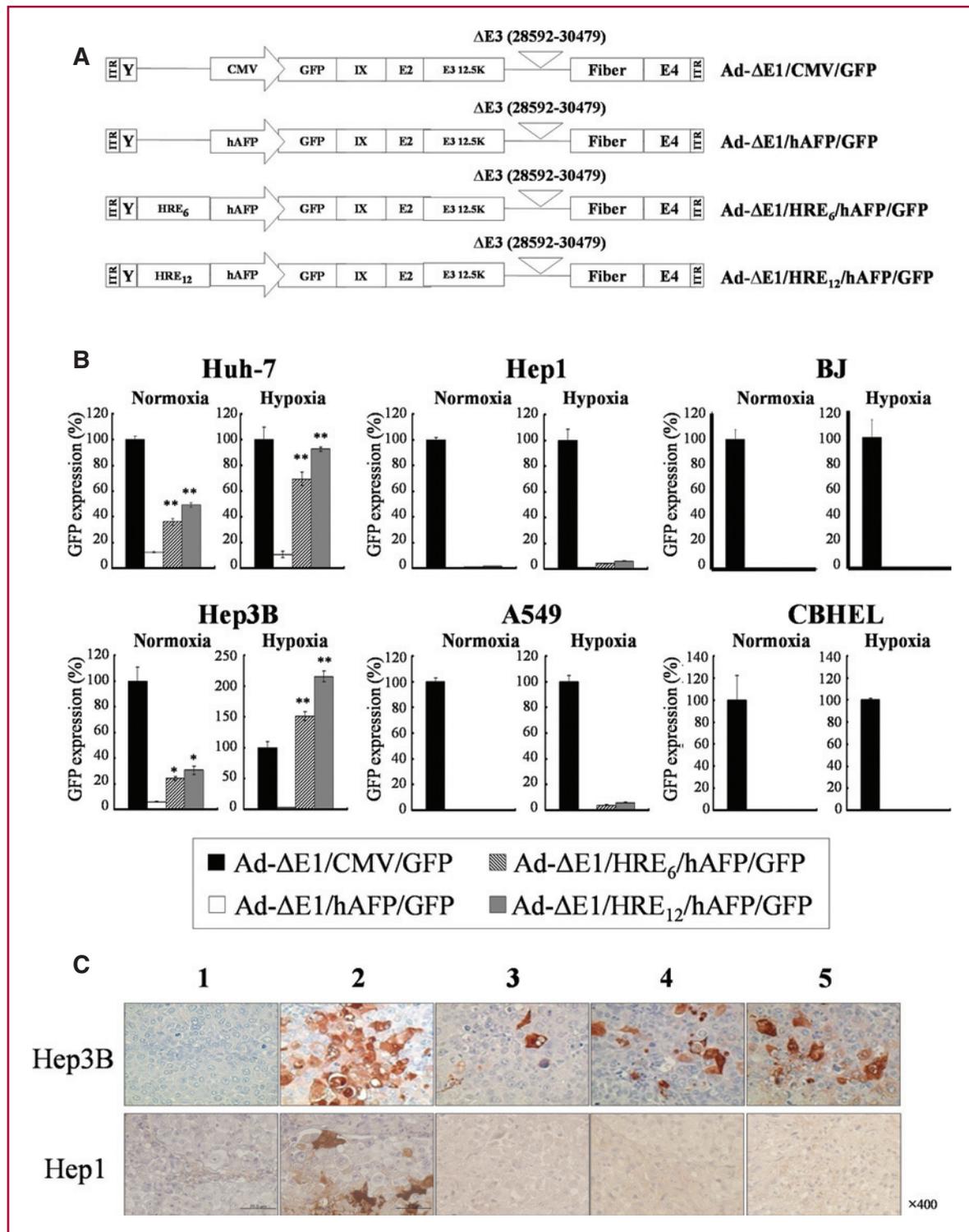
Fig. 1. HREs and hAFP promoter activity and selectivity test by replication-incompetent Ads *in vitro* and *in vivo*. A, GFP-expressing replication-incompetent Ads; Ad-ΔE1/CMV/GFP, Ad-ΔE1/hAFP/GFP, Ad-ΔE1/HRE$_6$/hAFP/GFP, and Ad-ΔE1/HRE$_{12}$/hAFP/GFP. B, all cells were transduced with each Ad (Huh-7, Hep3B, and A549 at 2,000 VPs; Hep1 and CBHEL at 5,000 VPs; BJ at 10,000 VPs) and incubated under normoxia or hypoxia. The transcriptional activity of CMV promoter was set as 100% in each cell line. Error bars represent ± SE. *, $P < 0.05$ versus Ad-ΔE1/hAFP/GFP treatment; **, $P < 0.01$ versus Ad-ΔE1/hAFP/GFP treatment. C, replication-incompetent Ads were intratumorally injected to Hep3B and Hep1 tumors. The tumor sections were stained by anti-GFP antibody. GFP appeared as brown color in tumor sections. 1, PBS; 2, Ad-ΔE1/CMV/GFP; 3, Ad-ΔE1/hAFP/GFP; 4, Ad-ΔE1/HRE$_6$/hAFP/GFP; 5, Ad-ΔE1/HRE$_{12}$/hAFP/GFP.

HREs/hAFP-controlled replication-incompetent Ads in different cell lines (the AFP levels of HCC; Huh-7, high; Hep3B and HepG2, moderate; Hep1, negative). The hAFP promoter exhibited specific GFP expression in AFP-positive HCCs as expected. In Huh-7, AFP-expressing HCC, Ad-ΔE1/hAFP/GFP expressed 13% and 10% of Ad-ΔE1/CMV/GFP under normoxia and hypoxia, respectively. In marked contrast, the addition of HREs augmented hAFP-driven activity to 36% and 69% by Ad-ΔE1/HRE$_6$/hAFP/GFP, under normoxia and hypoxia, respectively, and the Ad-ΔE1/HRE$_{12}$/hAFP/GFP exhibited 48% and 93% of Ad-ΔE1/CMV/GFP. Together, these results indicated that in Huh-7, the incorporation of HREs augmented gene expression 7- to 9-fold under hypoxia. Similar results were observed in Hep3B, another AFP-positive HCC. Ad-ΔE1/HRE$_6$/hAFP/GFP and Ad-ΔE1/HRE$_{12}$/hAFP/GFP exhibited 4- and 5-fold increases, respectively, relative to Ad-ΔE1/hAFP/GFP in normoxia. Surprisingly, HRE-integrated vectors achieved expression levels, exceeding that of the Ad-ΔE1/CMV/GFP in hypoxia, as the activity of Ad-ΔE1/HRE$_6$/hAFP/GFP and Ad-ΔE1/HRE$_{12}$/hAFP/GFP in Hep3B was 151% and 215% of that of Ad-ΔE1/CMV/GFP, respectively (Fig. 1B). The transcriptional activity of hAFP and HREs/hAFP seemed to be very low in AFP-negative cancer cell lines, Hep1 and A549, whereas a slight increase in GFP expression was observed under hypoxia. Importantly, negligible expression was seen in normal cells (BJ and CBHEL). Overall, the incorporation of HREs exhibited selective transcriptional activation in AFP-positive HCCs and further augmented the levels of expression under hypoxia, without affecting promoter selectivity.

After confirming the selective activity of the hAFP and HREs/hAFP promoter, the activity of these vectors in 2 HCC tumor models was examined (Fig. 1C). As shown, GFP expression derived from hAFP and HREs/hAFP promoter was detected only in Hep3B tumors but not in Hep1 tumors, an AFP-negative HCC. Parallel to the *in vitro* results, HRE$_6$- and HRE$_{12}$-incorporated hAFP constructs exhibited augmented expression over vector with hAFP alone. These results reaffirm that the designed specific expression control of the hAFP promoter and the augmentation effects of HREs remain functional in Ad vectors for *in vivo* applications in tumor xenografts.

Induction of CPE by HREs

Given that the hAFP and HREs could achieve specific and augmented gene expression controls in replication-deficient Ads, we proceed to use these elements to construct a series of oncolytic Ads (Fig. 2A). We first determined whether these oncolytic Ads could achieve cytotoxic activity in an AFP expression–dependent manner. As shown in Fig. 2B and Supplementary Fig. S2A, hAFP- and HREs/hAFP-driven oncolytic Ads exhibited selective cytotoxicity in AFP-positive HCCs. For example, in Hep3B cells, Ad-HRE$_6$/hAFPΔ19 exhibited 5- and 10-fold stronger cytotoxicity over Ad-hAFPΔ19 under normoxia and hypoxia, respectively. This augmentation was further increased with Ad-HRE$_{12}$/hAFPΔ19 to 7- and 20-fold. Negligible cytotoxi-

city was seen with the hAFP alone in other cell lines. Low-level cytotoxicity was observed with the HREs/hAFP in other cancer cell lines at higher MOIs, which likely attributed to hypoxia. No cytotoxicity was seen in normal cell lines in normoxia or hypoxia.

To further validate the cell-killing effects of the oncolytic Ads, cell viability assays were carried out at various time points (Fig. 2C; Supplementary Fig. S2B). Viability of mock-infected cells was set as 100% in each cell line. Again, Ad-hAFPΔ19, Ad-HRE$_6$/hAFPΔ19, and Ad-HRE$_{12}$/hAFPΔ19 exhibited cytotoxicity only in AFP-positive HCCs. These effects were further enhanced under hypoxia, depending on the number of HREs. Moreover, the IC$_{50}$ on Hep3B cell line was determined, as followed by Ad-ΔE1B19, 5 VPs; Ad-hAFPΔ19, 692 VPs; Ad-HRE$_6$/hAFPΔ19, 143 VPs; and Ad-HRE$_{12}$/hAFPΔ19, 104 VPs in normoxia. In hypoxic condition, the IC$_{50}$ was Ad-ΔE1B19 5 VPs; Ad-hAFPΔ19, 553 VPs; Ad-HRE$_6$/hAFPΔ19, 58 VPs; and Ad-HRE$_{12}$/hAFPΔ19, 22 VPs. In Hep1 cells, weak cytotoxic effects were observed with the vectors with HREs under hypoxia. In contrast, Ad-ΔE1B19 exhibited cytotoxicity in all other cell lines under both normoxia and hypoxia. From these experiments, we have shown that the hAFP promoter specifically controls expression of E1A proteins for viral replication in AFP-positive HCCs. In addition, incorporation of the HREs successfully augmented the CPE, especially under hypoxia.

Enhanced antitumor effect in the subcutaneous model

To evaluate and compare the antitumoral effects of oncolytic Ads, the growth of Hep3B tumors was monitored following intratumoral injection of the Ads. Figure 3A shows that tumor growth was suppressed by all viruses administered. The Ad-hAFPΔ19 showed 71% growth suppression (707.5 $\pm$ 302.2 mm^3) compared with PBS-injected tumors (2,437.0 $\pm$ 734.4 mm^3) on day 26. Ad-HRE$_6$/hAFPΔ19 and Ad-HRE$_{12}$/hAFPΔ19 exhibited much stronger tumor growth suppression, with tumor sizes of 126.3 $\pm$ 66.9 and 23.7 $\pm$ 16.4 mm^3, which were 5% and 1% the size of the sham-treated tumor, respectively. Particularly, growth suppression by Ad-HRE$_{12}$/hAFPΔ19 was comparable with the potent Ad-ΔE1B19 (39.2 $\pm$ 19.0 mm^3). Similar therapeutic effects were observed in a second Hep1 tumor model (Supplementary Fig. S3). Parallel to the results in cell culture experiments, insertion of HREs into Ad-hAFPΔ19 resulted in augmented *in vivo* tumoricidal activity that rivaled the most potent replication-competent Ad in our hand, Ad-ΔE1B19. To elucidate viral replication of these oncolytic viruses, we conducted immunohistochemical staining for Ad hexon protein in the tumor. Hypoxic regions of the tumor were also identified by pimonidazole staining. As shown in Fig. 3B, Ad hexon protein was detected in tumors treated with replication-competent Ads. As expected, the localization of Ad-HRE$_6$/hAFPΔ19 and Ad-HRE$_{12}$/hAFPΔ19 progeny VPs was overlapped with hypoxic regions, in addition to the normoxic regions, showing that the insertion of HREs can overcome the suppressed Ad replication in hypoxic condition. In marked contrast, VPs of Ad-ΔE1B19 and Ad-hAFPΔ19
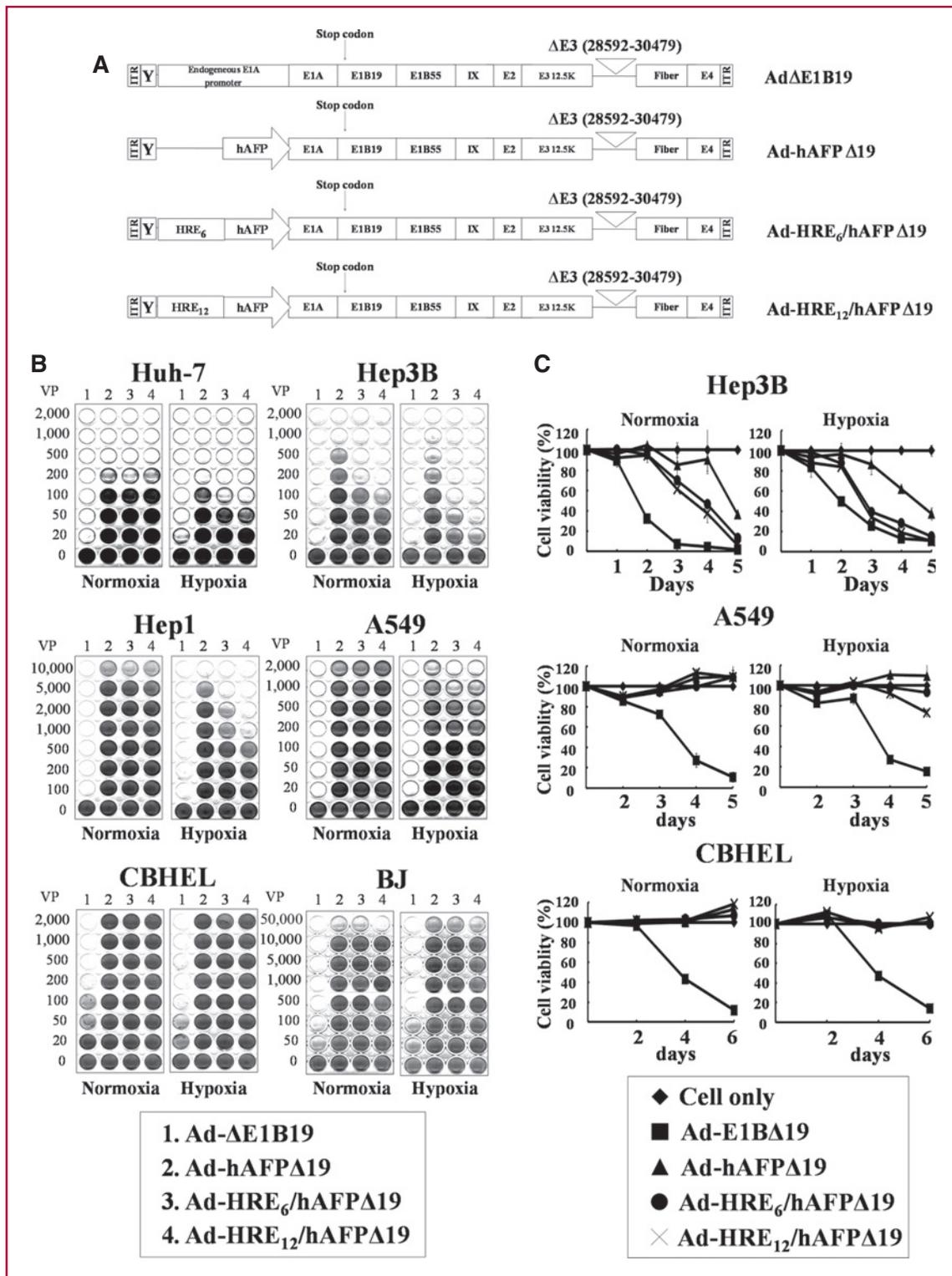
Fig. 2. *In vitro* cytotoxicity assay by HREs-hAFP oncolytic Ads. A, Ad-ΔE1B19 contains intact E1A and E1B55k. Other 3 vectors use hAFP promoter to drive E1A and 6 or 12 HREs are fused, Ad-hAFPΔ19, Ad-HRE₆/hAFPΔ19, and Ad-HRE₁₂/hAFPΔ19, respectively. B, cells were infected with replication-competent Ads at various VPs ranging from 20 to 50,000 and incubated under normoxia or hypoxia. Cells were thereafter incubated up to 17 days until being fixed and stained. C, cells were infected with Ad-ΔE1B19 (■), Ad-hAFPΔ19 (▲), Ad-HRE₆/hAFPΔ19 (●), or Ad-HRE₁₂/hAFPΔ19 (×) at the following VPs (50 VPs for Hep3B; 100 VPs for A549; 2,000 VPs for CBHEL) per cell. ♦, untreated cells. Uninfected cells were calculated as 100% at the same time points.

Fig. 3. *In vivo* tumor growth inhibition by HCC-targeted oncolytic Ads and immunohistochemical analysis in subcutaneous tumor xenografts. A, Hep3B tumor growth was monitored following the intratumoral administration of vectors. They received PBS (♦, filled diamond, $n = 6$), Ad-ΔE1B19 (■, filled square, $n = 6$), Ad-hAFPΔ19 (▲, filled triangle, $n = 6$), Ad-HRE$_6$/hAFPΔ19 (●, filled circle, $n = 6$), or Ad-HRE$_{12}$/hAFPΔ19 (×, $n = 6$) on days 0, 2, and 4. Tumor sizes are presented as means $\pm$ SEM. *, $P < 0.05$ versus Ad-hAFPΔ19 treatment; **, $P < 0.01$ versus PBS-treated group. B, tumor sections were stained by anti-Ad hexon antibody to examine virus replication (green). Antipimonidazole antibody was used to see the hypoxic regions (red). Both normoxic and hypoxic regions were represented.
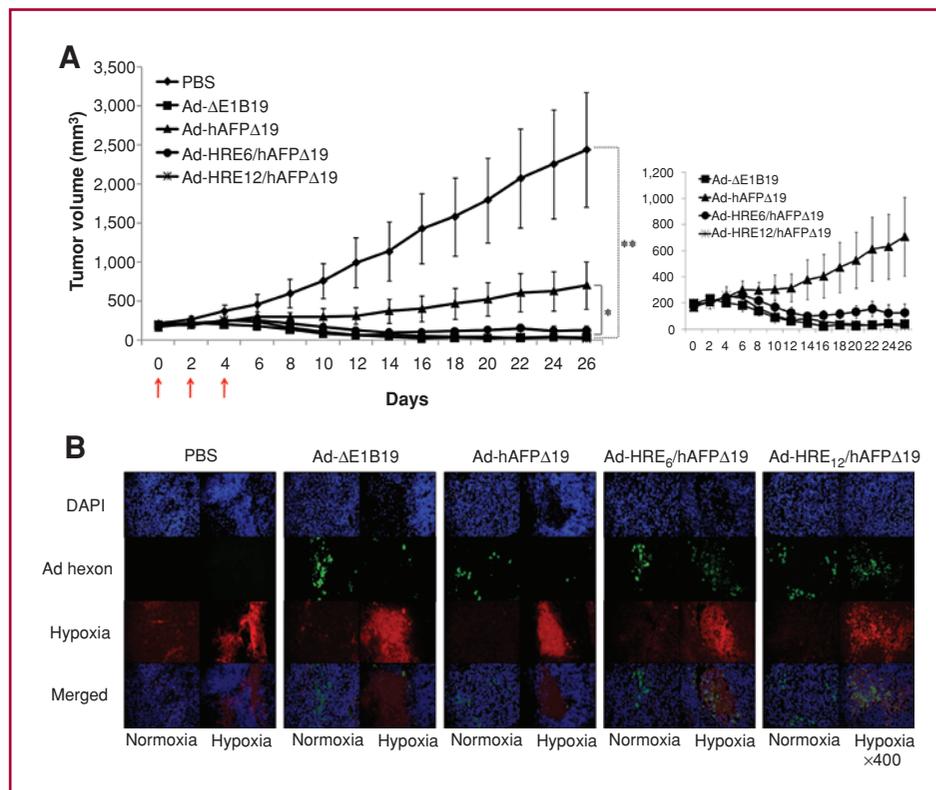
were not detected in hypoxic condition, implying that viral replication was inhibited in hypoxic tumor region. These results suggest that the insertion of HREs not only augmented antitumor activity of oncolytic Ads but also concentrated viral replication in hypoxia of tumors.

Therapeutic efficacy in orthotopic HCC after systemic administration

Following successful treatment of subcutaneous HCCs, we decided to evaluate the therapeutic efficacy in orthotopic liver cancer. In this experiment, we utilized 2 noninvasive methods to monitor tumor growth that includes bioluminescence imaging and serum AFP levels. As shown in Fig. 4A, tumors continued to grow for 4 weeks in PBS-treated mice. In contrast, mice treated with Ad-hAFPΔ19 and Ad-HRE$_{12}$/hAFPΔ19 exhibited significantly slower tumor growth rates. At 4 weeks posttreatment, the increase in total flux in Ad-hAFPΔ19- and Ad-HRE$_{12}$/hAFPΔ19–treated animals averaged 8.5- and 3.2-fold higher than the initial measurement, indicating 45.7% and 86.3% growth suppression, respectively (Fig. 4B). By tumor weight measurement at 4 weeks after treatment, suppression of tumor growth was 56.9% and 86.7% by Ad-hAFPΔ19 and Ad-HRE$_{12}$/hAFPΔ19, respectively (Fig. 4C). By the serum marker AFP, the average increase in sham-treated mice was 107-fold, whereas Ad-hAFPΔ19 and Ad-HRE$_{12}$/hAFPΔ19 treatment suppressed the AFP levels to 41.2% and 18.6% of control, respectively (Fig. 4D). As shown in Fig. 5A, Hep3B ortho-

topic liver tumor volume was smaller in response to treatment with Ad-HRE$_{12}$/hAFPΔ19 than either PBS or Ad-hAFPΔ19 treatment. Immunohistochemical analyses of tumor sections revealed higher expression of E1A in Ad-HRE$_{12}$/hAFPΔ19–treated tumors than in Ad-hAFPΔ19–treated tumors (Fig. 5B). Moreover, as shown in Fig. 5C, there is a close association of VPs (hexon staining in green) and hypoxia (pimonidazole staining in red) in Ad-HRE$_{12}$/hAFPΔ19–treated tumors. These results suggest that the inserted HRE$_{12}$ augments transcriptional activity of HCC-specific hAFP promoter, thus enabling Ad-HRE$_{12}$/hAFPΔ19 to achieve not only more potent oncolytic activity than the Ad-hAFPΔ19 virus but also in a hypoxia-responsive and AFP-targeted manner.

Reduced immune response and toxicity after systemic treatment of Ad-HRE$_{12}$/hAFPΔ19 oncolytic Ads

To analyze immune response and toxicity after systemic treatment of Ads, the levels of IL-6, AST, and ALT in serum were determined. At 6 hours after systemic viral injection, we observed remarkably enhanced IL-6 expression in Ad-ΔE1B19–treated group (156.63 ± 26.14 pg/mL) that was 8-fold above baseline level in PBS-treated group (19.83 ± 1.46 pg/mL). In marked contrast, the level of IL-6 was not markedly increased in Ad-HRE$_{12}$/hAFPΔ19 group (30.54 ± 2.35 pg/mL) compared with baseline level (Fig. 6A). Elevated serum transaminase levels were also detected in animals 3 days after treatment with Ad-ΔE1B19 (ALT, $1,625.6 \pm 434.3$ U/L; AST, $1,514.2 \pm 464.7$ U/L), whereas
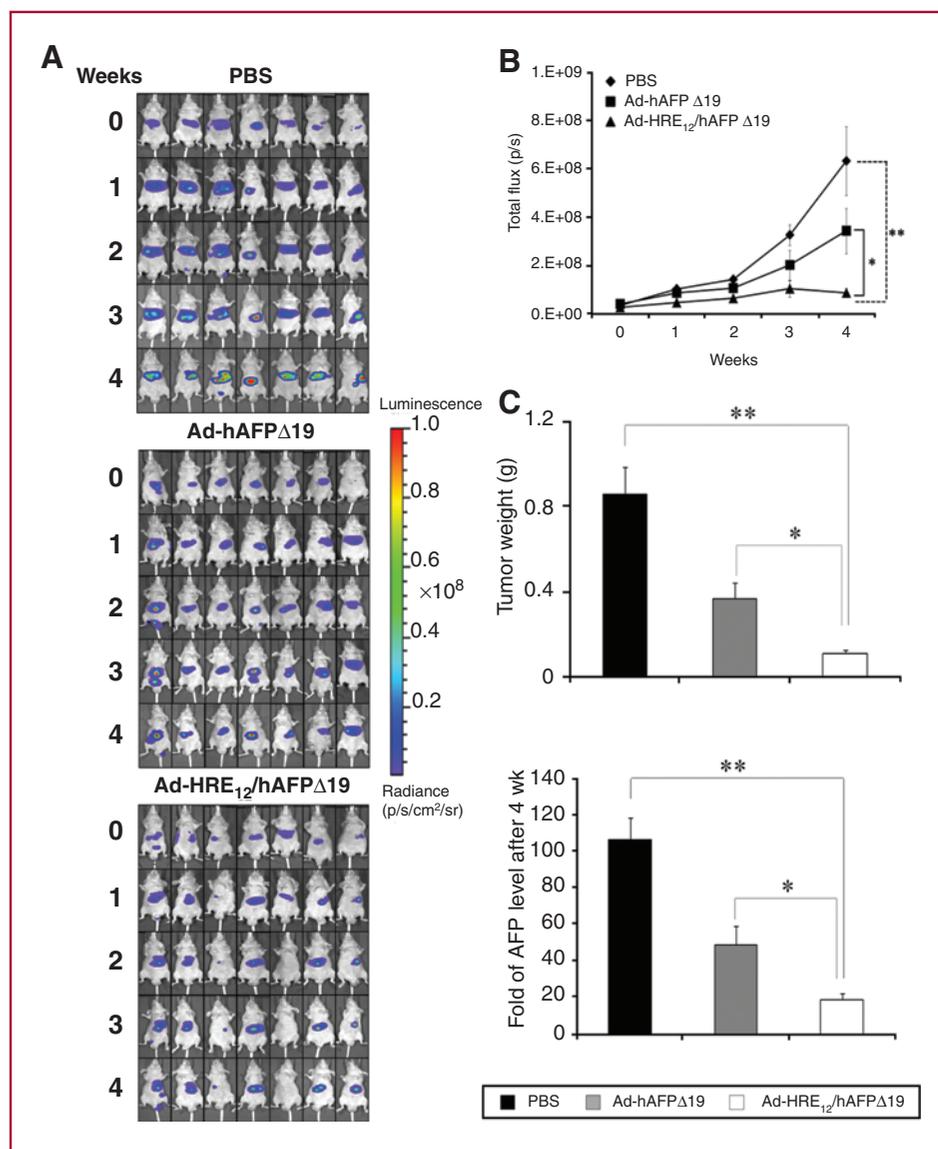
Fig. 4. *In vivo* tumor growth inhibition by HCC-targeted oncolytic Ads in liver orthotopic tumor xenografts. A, Hep3B tumor was monitored through optical imaging. At 15 days after tumor establishment, each vector was intravenously injected. Treatments included PBS ($n = 7$) as mock, Ad-hAFPΔ19 ($n = 7$), and Ad-HRE$_{12}$/hAFPΔ19 ($n = 7$); 1×10^{10} VPs, 3 time injection on days 0, 2, and 4. Firefly luciferase expression was monitored every week following the treatments. B, average optical signal intensity is shown by photons (p) acquired per second (s) in regions of interest. C, tumor weights were measured and plotted. D, fold increase of the serum AFP level was assessed by ELISA, dividing the levels at 4 weeks after last treatment by the levels before the treatment. *, $P < 0.05$ versus Ad-hAFPΔ19 treatment; **, $P < 0.01$ versus PBS treatment.

the liver enzyme levels in all Ad-HRE$_{12}$/hAFPΔ19–injected mice were in the normal range (ALT, 7–227 U/L; AST, 37–329 U/L). From H&E staining of organs in Fig. 6C, we detected tissue damage by the treatment of Ad-ΔE1B19 in lung, liver, and kidney. However, no abnormalities were observed in Ad-HRE$_{12}$/hAFPΔ19–injected group. Taken together, these results support that Ad-HRE$_{12}$/hAFPΔ19 has a potent antitumor activity with no inflammatory immune response and normal tissue toxicity.

Discussion

HCC, the most common form of the liver cancer, is known to be highly resistant to chemotherapy and radiotherapy. Because of its poor prognosis, an alternative approach to combat HCCs is urgently needed. To this end, we have worked to develop a safe and efficient HCC-targeted oncolytic Ad by utilizing the hAFP promoter. To date, a number of gene therapy strategies have utilized the AFP promoter to target HCCs. For instance, it has been used to drive the expression of *HSV-TK* suicide gene (23, 24). We and others have also incorporated the AFP promoter into an oncolytic Ad (25–27). Although these studies could show HCC-restricted transgene expression by the hAFP promoter, limited therapeutic efficacy was achieved. We postulate that this limited efficacy is most likely due to low transcriptional activity by the hAFP promoter. Hence, we integrated HREs into our oncolytic system in order to augment the transcriptional level of the AFP promoter.

Hypoxia is a process that is regulated by the transcription factor HIF-1, which activates gene expression by binding to an HRE (28). In rapidly growing malignant tumors and their metastases, hypoxia is a very common phenomenon.
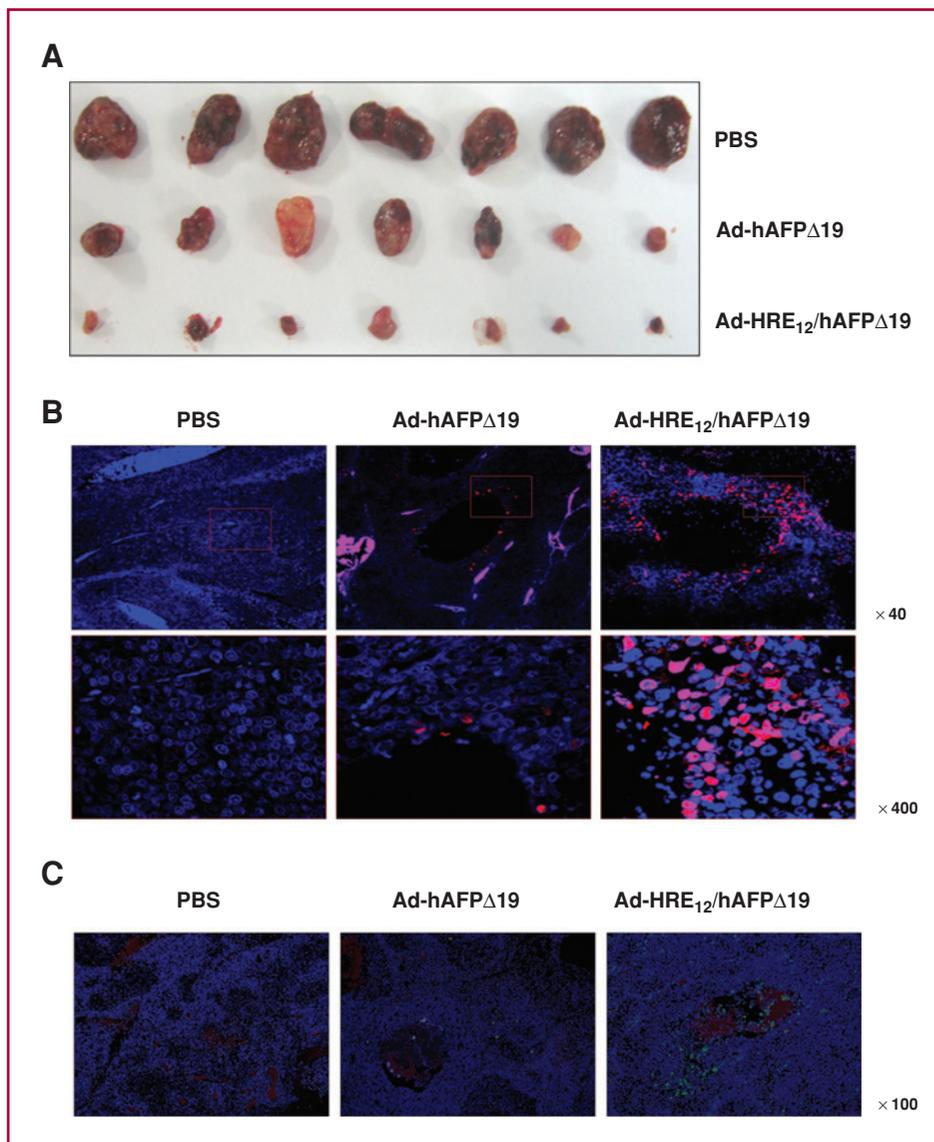
Fig. 5. The photograph and immunohistochemistry of liver orthotopic model. A, picture of Hep3B liver cancer on orthotopic model. At 4 weeks after treatment, mice were sacrificed, and tumor tissues were harvested. B, viral protein (E1A) was examined on the tumor sections obtained from liver orthotopic model of Hep3B xenografts. Sections were stained with Ad E1A (red) and DAPI (blue) in 2 different magnifications. C, relationships between hexon and hypoxia were examined, stained with hexon-specific Ab (green) and pimonidazole (red).

Hence, a favorable tumor-targeting strategy is to use HRE to drive transgene expression (29–32). Of interest, several physiologic conditions triggered under hypoxia can specifically interfere with hAFP promoter–driven oncolytic processes. For example, a negative element in the AFP gene regulatory region has been reported to counter the actions of HIF-1α and specifically worked to repress its expression under hypoxia (33). In addition, hypoxia is known to have a direct impact on oncolytic Ad gene therapy by suppressing viral replication through reduced E1A protein expression (34, 35). In this study, we fused HREs to the hAFP promoter to control Ad replication in our oncolytic system. We anticipate 3 potential advantages to this strategy. First, the HREs can serve as an enhancer to augment the transcriptional activity of the hAFP promoter. Second, the HREs can act to achieve added tumor selectivity by targeting the

hypoxic environment encountered in tumors. Third, as mentioned earlier, AFP expression in HCC is not ubiquitous but is approximately 70%. The inclusion of HRE and hypoxia targeting could broaden the therapeutic efficacy of our oncolytic virus to impact AFP-negative or AFP-low HCCs.

We first compared the transcriptional activity and selectivity of hAFP and HREs/hAFP promoter constructs in a systematic manner. Our results consistently showed that HREs/hAFP promoter–driven systems retained selectivity by restricting expression in AFP-positive HCCs, while remaining silent in normal cells. The HRE-mediated transcriptional augmentation occurred as expected in a hypoxia-responsive manner, and was proportional to the number of repeats of HRE. We observed HRE-mediated transcriptional augmentation in both high and moderate
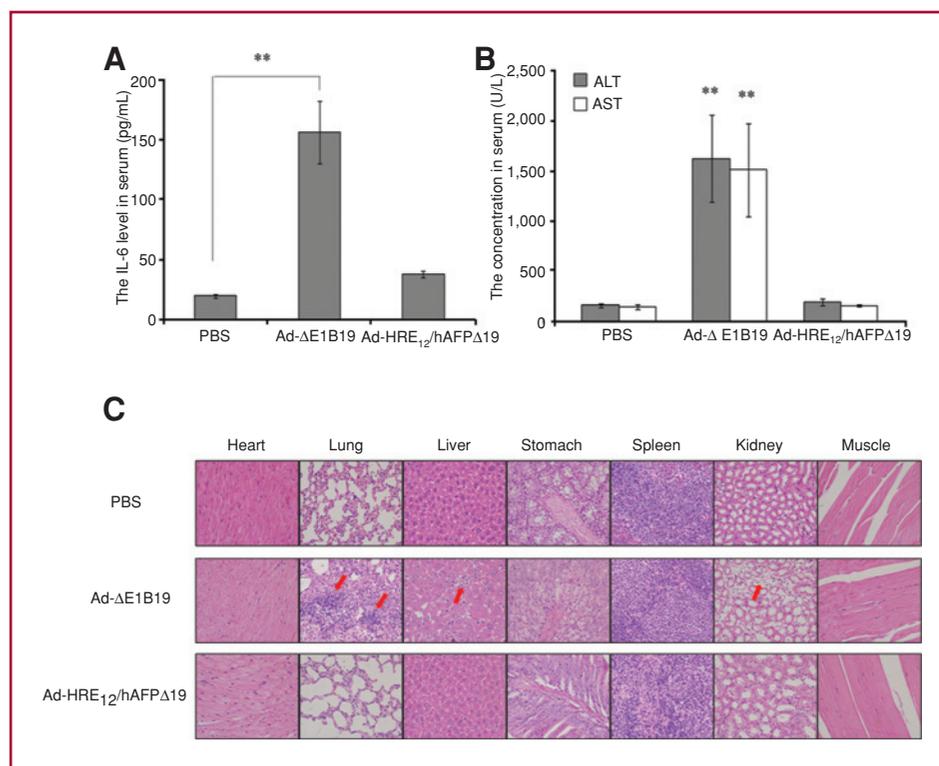
Fig. 6. Evaluation of inflammatory immune response, liver toxicity, and tissue damage after intravenous administration of oncolytic Ads. A, induction of IL-6 inflammatory cytokine. At 6 hours after systemic injection of PBS, Ad-ΔE1B19, or Ad-HRE$_{12}$/hAFPΔ19 (2×10^{10} VPs), serum level of IL-6 was measured by ELISA. **, $P < 0.01$ versus PBS. B, assessment of hepatotoxicity. Measurement of serum ALT and AST levels at 72 hours following intravenous administration of Ad-ΔE1B19 or Ad-HRE$_{12}$/hAFPΔ19. **, $P < 0.01$ versus PBS and Ad-HRE$_{12}$/hAFPΔ19. C, assessment of tissue histopathology. Photomicrographs of representative H&E-stained organs (heart, lung, liver, stomach, spleen, kidney, and muscle) at 72 hours after intravenous injection of each Ad preparation.

AFP-expressing cells. Interestingly, this augmentation was more robust in moderate AFP-expressing cells. For instance, in high AFP-expressing Huh-7 cells, the vector with 12 repeats of HRE (Ad-ΔE1/HRE$_{12}$/hAFP/GFP) exhibited nearly 10-fold higher expression than the vector with hAFP alone in hypoxia. In moderate AFP-expressing Hep3B cells, the same vector exhibited more than 20-fold higher activity, even higher than those of CMV promoter. However, this dramatic increase in HRE-inserted AFP promoter activity over CMV promoter was not observed in Hep3B tumor model (Fig. 1C). Given this discrepancy between *in vitro* and *in vivo* tumor models, one possibility brought forth is that the concentration of oxygen is variable depending on the size and area of tumor tissues whereas the percentage of oxygen in *in vitro* experiments can be tightly controlled using hypoxia chamber.

The specific and regulated expression profiles displayed by the chimeric HREs/hAFP reporter constructs encouraged us to use the same approach to develop oncolytic Ad vectors in which the *E1A* gene is regulated by the HREs/hAFP promoter. We thoroughly characterized and compared the CPEs of the novel oncolytic viruses, including the Ad-hAFPΔ19, Ad-HRE$_6$/hAFPΔ19, and Ad-HRE$_{12}$/hAFPΔ19. Again, the therapeutic capabilities of the hAFP-targeted oncolytic virus recapitulated the promising findings that were observed in reporter vectors. Specifically, incorporation of HREs, especially the HRE$_{12}$, upstream of the hAFP promoter greatly accentuated the CPEs of the oncolytic Ad in both high and moderate AFP-expressing HCCs and even

in AFP-negative Hep1 cells under hypoxia. Remarkably, the Ad-HRE$_{12}$/hAFPΔ19 could achieve cell-killing activity that rivals that of the potent but non–cancer-selective replicating Ad, Ad-ΔE1B19, while also maintaining HCC cell-discriminating ability in an exquisite AFP- and hypoxia-restricted manner.

We further tested the therapeutic activities in preclinical models of HCC, a subcutaneous and an orthotopic Hep3B xenograft model. We were able to clearly observe the superior therapeutic efficacy of systemically administered Ad-HRE$_{12}$/hAFPΔ19 therapy in liver-implanted Hep3B tumor model. Because of the deep intra-abdominal location of the orthotopic liver tumors, we applied several methods to track and assess tumor growth including photon flux measured by bioluminescent imaging of the luciferase-marked Hep3B cells, serum AFP levels, and endpoint tumor weight. The results from these 3 methods correlated very well and showed more effective inhibition of tumor growth by Ad-HRE$_{12}$/hAFPΔ19 over Ad-hAFPΔ19. We anticipate that intravenous administration would disperse Ads more evenly within the tumor compared with intratumoral injection and would deliver the vector preferential to well-vascularized, normoxic areas within the tumor. Yet, detail histologic analyses revealed an increased magnitude and prevalent localization of progeny virus in hypoxic region of tumors after systemic delivery of Ad-HRE$_{12}$/hAFPΔ19 compared with that of Ad-hAFPΔ19. These data are consistent with the notion that the incorporated HREs are directing heightened viral replication and tumor lysis compared with

Ad-hAFPΔ19. The remarkable selectivity of Ad-HRE$_{12}$/hAFPΔ19 coupled to its reduced inflammatory immune response and tissue toxicity supports the idea that this chimeric oncolytic virus could achieve both potent and safe therapeutic outcomes in treating HCCs.

A previous report by Ido and colleagues (36) has shown that fusing an HRE from the *VEGF* gene to the AFP promoter successfully increased the expression and therapeutic efficacy of a retroviral vector–mediated suicide gene therapy strategy. The approaches taken in this study differ from the prior report in several aspects. First, compared with the proximal 0.3-kb hAFP promoter utilized in the previous study, the current hAFP promoter is more extensive, consisting of an upstream 2-kb enhancer region fused to the 169-bp proximal promoter, and is more potent and selective. Second, we expanded the number of incorporated HREs greatly to 6 and 12 copies. A clear copy number–dependent augmentation of activity was observed in our study. Third, we incorporated the HRE-mediated transcriptional augmentation in the context of a replicating oncolytic virus, which is likely to be much more potent than the replication-deficient retroviral-mediated gene therapy strategy reported. To our knowledge, this is the first study reporting on the use of the improved chimeric HREs/hAFP promoters to drive an oncolytic Ad therapeutic system. We thoroughly tested and showed the unique ability of the most advanced vector Ad-HRE$_{12}$/hAFPΔ19 to unleash its potent cytotoxic activity in both a tumor environment–selective and a liver tumor–specific manner.

Several oncolytic Ad vectors are being tested in ongoing clinical trials. For instance, China recently approved the world's first oncolytic Ad, HB101, as a cancer therapeutic agent (http://www.bgwicc.org.cn/english/2437.html). This HB101 vector, a kin to the E1B 55-kD-deleted virus Onyx-015 (37), was developed by China's Sunway Biotech Company. Moreover, we have also observed promising results in early clinical tests in patients with solid tumors, using an oncolytic Ad regulated by the cancer-selective modified TERT promoter (38) developed by our group. Current oncolytic Ad therapy is mainly delivered by intratumoral injection. Because of limited intratumoral viral spread, the efficacy of this mode of therapy might be suboptimal. An important direction to advance oncolytic Ads for future clinical applications is to develop novel vectors capable of targeting both primary and metastatic cancer lesions by systemic delivery. This approach could achieve more evenly distributed gene transfer within the tumors and more effective therapeutic outcomes, as shown in this study. The work presented here shows the feasibility of targeting and treating metastatic tumors in the liver by systemic oncolytic viral therapy. The success of this approach was aided by the well-documented preferential vector delivery to the liver after systemic delivery (39–41). This study shows the promising results of using the exquisite transcriptional selectivity of HREs/hAFP promoter to direct oncolytic viral therapy. Potent and cancer-specific transcriptional regulation constitutes an important fundamental technology to integrate further surface engineering to achieve safe, effective, and targeted oncolytic viral therapy in the medical management of aggressive HCCs.

Disclosure of Potential Conflicts of Interest

No potential conflicts of interest were disclosed.

Grant Support

References

1. Parkin DM, Bray F, Ferlay J, Pisani P. Global cancer statistics, 2002. CA Cancer J Clin 2005;55:74–108.
2. Bosch FX, Ribes J, Diaz M, Cleries R. Primary liver cancer: worldwide incidence and trends. Gastroenterology 2004;127:S5–16.
3. Llovet JM, Burroughs A, Bruix J. Hepatocellular carcinoma. Lancet 2003;362:1907–17.
4. Liu TC, Kirn D. Gene therapy progress and prospects cancer: oncolytic viruses. Gene Ther 2008;15:877–84.
5. Roth JA, Cristiano RJ. Gene therapy for cancer: what have we done and where are we going?J Natl Cancer Inst 1997;89:21–39.
6. Gene therapy clinical trials worldwide. J Gene Med 2009. Available from: http://www.wiley.co.uk/genetherapy/clinical.
7. McConnell MJ, Imperiale MJ. Biology of adenovirus and its use as a vector for gene therapy. Hum Gene Ther 2004;15:1022–33.
8. Kanerva A, Hemminki A. Modified adenoviruses for cancer gene therapy. Int J Cancer 2004;110:475–80.
9. St George JA. Gene therapy progress and prospects: adenoviral vectors. Gene Ther 2003;10:1135–41.
10. Johnson M, Huyn S, Burton J, Sato M, Wu L. Differential biodistribution of adenoviral vector *in vivo* as monitored by bioluminescence imaging and quantitative polymerase chain reaction. Hum Gene Ther 2006;17:1262–9.
11. Wood M, Perrotte P, Onishi E, Harper ME, Dinney C, Pagliaro L, et al. Biodistribution of an adenoviral vector carrying the luciferase reporter gene following intravesical or intravenous administration to a mouse. Cancer Gene Ther 1999;6:367–72.
12. Vaha-Koskela MJ, Heikkila JE, Hinkkanen AE. Oncolytic viruses in cancer therapy. Cancer Lett 2007;254:178–216.
13. Green NK, Seymour LW. Adenoviral vectors: systemic delivery and tumor targeting. Cancer Gene Ther 2002;9:1036–42.
14. Kim J, Cho JY, Kim JH, Jung KC, Yun CO. Evaluation of E1B gene-attenuated replicating adenoviruses for cancer gene therapy. Cancer Gene Ther 2002;9:725–36.
15. Ko D, Hawkins L, Yu DC. Development of transcriptionally regulated oncolytic adenoviruses. Oncogene 2005;24:7763–74.

16. Debruyne EN, Delanghe JR. Diagnosing and monitoring hepatocellular carcinoma with alpha-fetoprotein: new aspects and applications. Clin Chim Acta 2008;395:19–26.

17. Sell S, Becker FF, Leffert HL, Watabe L. Expression of an oncodevelopmental gene product (alpha-fetoprotein) during fetal development and adult oncogenesis. Cancer Res 1976;36:4239–49.

18. Kew M. Alpha-fetoprotein in primary liver cancer and other diseases. Gut 1974;15:814–21.

19. Nakabayashi H, Hashimoto T, Miyao Y, Tjong KK, Chan J, Tamaoki T. A position-dependent silencer plays a major role in repressing alpha-fetoprotein expression in human hepatoma. Mol Cell Biol 1991;11:5885–93.

20. Yasuda H. Solid tumor physiology and hypoxia-induced chemo/radioresistance: novel strategy for cancer therapy: nitric oxide donor as a therapeutic enhancer. Nitric Oxide 2008;19:205–16.

21. Bertout JA, Patel SA, Simon MC. The impact of O_2 availability on human cancer. Nat Rev Cancer 2008;8:967–75.

22. Harris AL. Hypoxia—a key regulatory factor in tumour growth. Nat Rev Cancer 2002;2:38–47.

23. Kanai F, Shiratori Y, Yoshida Y, Wakimoto H, Hamada H, Kanegae Y, et al. Gene therapy for alpha-fetoprotein-producing human hepatoma cells by adenovirus-mediated transfer of the herpes simplex virus thymidine kinase gene. Hepatology 1996;23:1359–68.

24. Ido A, Nakata K, Kato Y, Nakao K, Murata K, Fujita M, et al. Gene therapy for hepatoma cells using a retrovirus vector carrying herpes simplex virus thymidine kinase gene under the control of human alpha-fetoprotein gene promoter. Cancer Res 1995;55:3105–9.

25. Takahashi M, Sato T, Sagawa T, Lu Y, Sato Y, Iyama S, et al. E1B-55K-deleted adenovirus expressing E1A-13S by AFP-enhancer/promoter is capable of highly specific replication in AFP-producing hepatocellular carcinoma and eradication of established tumor. Mol Ther 2002;5:627–34.

26. Kim J, Lee B, Kim JS, Yun CO, Kim JH, Lee YJ, et al. Antitumoral effects of recombinant adenovirus YKL-1001, conditionally replicating in alpha-fetoprotein-producing human liver cancer cells. Cancer Lett 2002;180:23–32.

27. Ohashi M, Kanai F, Tateishi K, Taniguchi H, Marignani PA, Yoshida Y, et al. Target gene therapy for alpha-fetoprotein-producing hepatocellular carcinoma by E1B55k-attenuated adenovirus. Biochem Biophys Res Commun 2001;282:529–35.

28. Ke Q, Costa M. Hypoxia-inducible factor-1 (HIF-1). Mol Pharmacol 2006;70:1469–80.

29. Dachs GU, Patterson AV, Firth JD, Ratcliffe PJ, Townsend KM, Stratford IJ, et al. Targeting gene expression to hypoxic tumor cells. Nat Med 1997;3:515–20.

30. Binley K, Askham Z, Martin L, Spearman H, Day D, Kingsman S, et al. Hypoxia-mediated tumour targeting. Gene Ther 2003;10:540–9.

31. Cho WK, Seong YR, Lee YH, Kim MJ, Hwang KS, Yoo J, et al. Oncolytic effects of adenovirus mutant capable of replicating in hypoxic and normoxic regions of solid tumor. Mol Ther 2004;10:938–49.

32. Post DE, Van Meir EG. A novel hypoxia-inducible factor (HIF) activated oncolytic adenovirus for cancer therapy. Oncogene 2003; 22:2065–72.

33. Mazure NM, Chauvet C, Bois-Joyeux B, Bernard MA, Nacer-Cherif H, Danan JL. Repression of alpha-fetoprotein gene expression under hypoxic conditions in human hepatoma cells: characterization of a negative hypoxia response element that mediates opposite effects of hypoxia inducible factor-1 and c-Myc. Cancer Res 2002;62:1158–65.

34. Shen BH, Hermiston TW. Effect of hypoxia on Ad5 infection, transgene expression and replication. Gene Ther 2005;12:902–10.

35. Pipiya T, Sauthoff H, Huang YQ, Chang B, Cheng J, Heitner S, et al. Hypoxia reduces adenoviral replication in cancer cells by downregulation of viral protein expression. Gene Ther 2005;12:911–7.

36. Ido A, Uto H, Moriuchi A, Nagata K, Onaga Y, Onaga M, et al. Gene therapy targeting for hepatocellular carcinoma: selective and enhanced suicide gene expression regulated by a hypoxia-inducible enhancer linked to a human alpha-fetoprotein promoter. Cancer Res 2001;61:3016–21.

37. Bischoff JR, Kirn DH, Williams A, Heise C, Horn S, Muna M, et al. An adenovirus mutant that replicates selectively in p53-deficient human tumor cells. Science 1996;274:373–6.

38. Kim E, Kim JH, Shin HY, Lee H, Yang JM, Kim J, et al. Ad-mTERT-delta19, a conditional replication-competent adenovirus driven by the human telomerase promoter, selectively replicates in and elicits cytopathic effect in a cancer cell-specific manner. Hum Gene Ther 2003;14:1415–28.

39. Jeong JS, Lee SW, Hong SH, Lee YJ, Jung HI, Cho KS, et al. Antitumor effects of systemically delivered adenovirus harboring trans-splicing ribozyme in intrahepatic colon cancer mouse model. Clin Cancer Res 2008;14:281–90.

40. Li ZY, Ni S, Yang X, Kiviat N, Lieber A. Xenograft models for liver metastasis: relationship between tumor morphology and adenovirus vector transduction. Mol Ther 2004;9:650–7.

41. Yin C, Lin Y, Zhang X, Chen YX, Zeng X, Yue HY, et al. Differentiation therapy of hepatocellular carcinoma in mice with recombinant adenovirus carrying hepatocyte nuclear factor-4alpha gene. Hepatology 2008;48:1528–39.

Clinical Cancer Research